approximation of the low-temperature phase of $NbTe_4$ and for the commensurate room-temperature structure of $TaTe_4$.

The project has been supported by a grant of the Deutsche Forchungsgemeinschaft, local support was given by the Materialwissenschaftliches Forschungszentrum der Universität Mainz. The authors thank J. C. Bennet (Waterloo, Ontario) who supplied the single crystals for comparative measurements.

References

BÖHM, H. & VON SCHNERING, H.-G. (1983). *Z. Kristallogr.* **162**, 26–27.
BÖHM, H. & VON SCHNERING, H.-G. (1985). *Z. Kristallogr.* **171**, 41–64.
BOSWELL, F. W. & PRODAN, A. (1986). *Phys. Rev. B*, **34**, 2979–2981.
BOSWELL, F. W., PRODAN, A. & BRANDON, J. K. (1983). *J. Phys. C*, **16**, 1067–1076.
BRONSEMA, K. D., VAN SMAALEN, S., DE BOER, J. L., WIGERS, G. A., JELLINEK, F. & MAHY, J. (1987). *Acta Cryst.* **B43**, 305–313.
BUDKOWSKI, A., PRODAN, A., MARINKOVIC, V., KUCHARCZYK, D., USZYNSKI, I. & BOSWELL, F. W. (1989). *Acta Cryst.* **B45**, 529–534.
EAGLESHAM, D. J., BIRD, D., WITHERS, R. L. & STEEDS, J. W. (1985). *J. Phys. C*, **18**, 1–11.
KUSZ, J. & BÖHM, H. (1992). *Z. Kristallogr.* **201**, 9–17.
KUSZ, J. & BÖHM, H. (1993). *Z. Kristallogr.* **208**, 187–194.
MAHY, J., VAN LANDUYT, J., AMELINCKX, S., BRONSEMA, K. D. & VAN SMAALEN, S.(1986). *J. Phys. C*, **19**, 5049–5069.
PACIOREK, W. A. & USZYNSKI, I. (1987). *J. Appl. Cryst.* **20**, 57–59.
PRODAN, A., BOSWELL, F. W., BENNET, J. C., CORBETT, J. M., VIDMAR, T., MARINKOWIC, V. & BUDKOWSKI, A. (1990). *Acta Cryst.* **B46**, 587–591.
SELTE, K. & KJEKSHUS, A. (1964). *Acta Chem. Scand.* **18**, 690–696.
SHELDRICK, G. M. (1976). *SHELX76. Program for Crystal Structure Determination*. Univ. of Cambridge, England.
SMAALEN, S. VAN, BRONSEMA, K. D. & MAHY, J. (1986). *Acta Cryst.* **B42**, 43–50.
ZUCKER, U. H., PERENTHALER, E., KUHS, W., BACHMANN, R. & SCHULZ, H. (1983). *J. Appl. Cryst.* **16**, 358–362.

Acta Cryst. (1994). **B50**, 655–662

Structure and Non-Linear Optical Properties of $KTiOAsO_4$

BY S. C. MAYO*

Clarendon Laboratory, Parks Road, Oxford OX1 3PU, England

P. A. THOMAS† AND S. J. TEAT

Department of Physics, University of Warwick, Coventry CV4 7AL, England

AND G. M. LOIACONO AND D. N. LOIACONO

Crystal Associates Inc., Waldwick, NJ 07463, USA

(*Received* 16 *February* 1994; *accepted* 2 *June* 1994)

Abstract

Refinements of the crystal structures of potassium titanyl arsenate, $KTiOAsO_4$, grown from a tungstate flux (1) and an arsenate flux (2), are reported. Crystal data at room temperature are: (1) $KTiOAsO_4$, orthorhombic, $Pna2_1$, $a = 13.138$ (2), $b = 6.582$ (1), $c = 10.787$ (2) Å, $Z = 8$, $R = 0.027$ for 2086 reflections with $I > 3\sigma(I)$; (2) $KTiOAsO_4$, orthorhombic, $Pna2_1$, $a = 13.130$ (2), $b = 6.581$ (1), $c = 10.781$ (1) Å, $Z = 8$, $R = 0.020$ for 2716 observed reflections with $I > 3\sigma(I)$. The values of the linear and non-linear optical susceptibilities for $KTiOAsO_4$ are discussed using the isostructural non-linear optical crystal $KTiOPO_4$ as a starting point. The observed increase in certain non-linear optical coefficients of $KTiOAsO_4$ is shown to derive principally from the increase in the linear refractive indices brought about by the substitution of phosphorus by arsenic in the structure.

Introduction

Potassium titanyl phosphate, $KTiOPO_4$ (KTP), and its analogues have been of interest for many years because of their suitability for non-linear optical applications (Zumsteg, Bierlein & Gier, 1976). In particular, KTP is known as a highly efficient frequency doubler for 1.06 μm radiation (Perkins & Fahlen, 1987). The isostructural analogue

* Present address: Research School of Chemistry, Australian National University, Canberra, ACT0200, Australia.
† Author for further correspondence.

$KTiOAsO_4$ (KTA) was initially reported to show a 60% higher effective coefficient for frequency doubling of 1.06 μm radiation (Bierlein, Vanherzeele & Ballman, 1989) than KTP itself. However, subsequent to this, other researchers were unable to reproduce this result; this was originally thought to be the result of using multi-domain crystals for the optical experiments. In fact, it has been shown that *pure* KTA does not phase-match for 1.06 μm radiation and that the original results were obtained with iron-doped crystals (Bierlein, Vanherzeele & Ballman, 1989; Cheng, Cheng, Bierlein, Zumsteg & Ballman, 1993). There still remains a query over whether pure KTA grows as single-domain or multi-domain crystals; Cheng *et al.* (1993) have reported that the addition of small amounts of Fe_2O_3, Sc_2O_3 and In_2O_3 to the flux is required to promote the growth of single-domain specimens.

Recently it has been shown (Cheng *et al.*, 1993) that some non-linear coefficients of KTA are indeed enhanced over those of KTP, although by only 20% or so. Despite the fact that KTA does not phase-match for 1.06 μm radiation, it remains applicable in other areas, for example, as a parametric oscillator material (Jani, Murray, Petrin, Powell, Loiacono & Loiacono, 1992) or as an electrooptic modulator crystal (Vanherzeele & Ballman, 1992). In an earlier structural study of KTA, El Brahimi & Durand (1986) reported that the AsO_4 tetrahedra are highly distorted compared with the PO_4 tetrahedra in KTP (Tordjman, Masse & Guitel, 1974). This was subsequently suggested to be the origin of the increased non-linear optical coefficients in KTA (Bierlein *et al.*, 1989). More recently, studies of $KTiO(P_{0.5}As_{0.5})O_5$ and $KTiO(P_{0.58}As_{0.42})O_4$ (KTAP) have been carried out using neutron powder diffraction (Crennell, Cheetham, Jarman, Thrash & Kaduk, 1992) and single-crystal X-ray diffraction (Thomas, Mayo & Watts, 1992), respectively. Compared with the crystal structures of KTP and the mixed compound KTAP, the published KTA structure of El Brahimi & Durand (1986) showed some anomalies, particularly in the TiO_6 octahedra.

The failure of structural models to account adequately for the observed optical non-linearity in KTA led us to examine the structural data again. In the original work, a very limited data set was collected, no absorption correction was made to the data and no mention was made of the use of anomalous scattering corrections to the scattering factors. The parameters obtained for the O atoms had large quoted errors and several thermal ellipsoids were anomalous, including those of the O atoms involved in the short Ti—O bonds. In view of this, we considered it necessary to collect structural data from these crystals again, particularly because the development of structural models for non-linear optical behaviour requires accurate structural data. X-ray diffraction, etching and second-harmonic generation measurements of KTA crystals grown from two different fluxes, arsenate and tungstate, both of which are used commercially, are reported here in an attempt to explain their physical properties.

Structure determination

Experimental detail

Crystals of KTA were grown from both a mixed tungstate/arsenate and a pure arsenate solvent. The mixed solvent was prepared by melting 2 mol each of K_2CO_3 and WO_3 with 1 mol of KH_2AsO_4 in a platinum crucible. The solution was saturated by adding 0.33 mol of previously prepared $KTiOAsO_4$ per mole of solvent, which resulted in a saturation temperature of 1153 K. The pure arsenate solvent was prepared by melting 4 mol of KH_2AsO_4 with 1 mol of K_2CO_3 to yield the composition $K_6As_4O_{13}$. The pure arsenate solvent was saturated at 1193 K at a concentration of 0.75 mol of $KTiOAsO_4$ per mole of $K_6As_4O_{13}$.

Large KTA crystals were grown using oriented seed crystals over the temperature ranges 1103–1153 K for the mixed and pure solvents, respectively. Cooling rates were incrementally increased from 1 to 4 K per day. Extensive details of these crystal growth procedures have been previously reported elsewhere (Loiacono, Loiacono, Zola, Stolzenberger, McGee & Norwood, 1992). Crystals in a range of sizes up to a maximum of $25 \times 30 \times 45$ mm were grown and found to be free of veils and other gross growth defects. Growth striae were clearly visible in crystals grown from the tungsten-based solvent.

Small fragments were cut from both crystals and were examined under the polarizing microscope. Suitable samples both from a tungstate- and an arsenate-grown crystal were mounted on a Stoe four-circle diffractometer for data collection. Details of the data collections and refinements are given in Table 1.*

Result of refinements

Both the refinements proceeded normally with the exception of an anomalously small temperature factor for Ti(2). Fourier difference maps revealed a small electron-density peak of *ca* 3 e $Å^{-3}$ adjacent to this site at the end of both refinements. Since absorption effects had been well accounted for by ψ-scans

* Lists of anisotropic displacement parameters and structure factors have been deposited with the IUCr (Reference: HA0133). Copies may be obtained through The Managing Editor, International Union of Crystallography, 5 Abbey Square, Chester CH1 2HU, England.

Table 1(*a*). *Details of data collection and refinement common to both tungstate- and arsenate-grown KTA*

M_r	241.92
D_x (Mg m^{-3})	3.45
Linear absorption coefficient (cm^{-1})	101.16
Diffractometer	Stoe Stadi-4
Radiation	Mo $K\alpha$
Scan type	ω 2θ
Range of data collection	2 unique sets and their Friedel opposites $2\theta = 3$ 70°
Intensity control	Every hour
Orientation control	Every 4 h
Absorption correction	Empirical φ-scans
Data reduction	*REDU*4[1] and *CRYSTALS*[2]
Refinement method	*FMLS* (*CRYSTALS*[2])
Weighting scheme	Robust resistant refinement: $w = w'x$ $[1 - (\Delta_F/6 \times \Delta_{F_{estimated}})^2]^2$ w' = third-order Chebychev weights
No. of parameters	153

(1) Stoe & Cie (1988); (2) Watkin, Carruthers & Betteridge (1985).

Table 1(*b*). *Remaining details of data collection and refinement for tungstate- and arsenate-grown* $KTiOAsO_4$

Crystal	$KTiOAsO_4$(W)	$KTiOAsO_4$(As)
Crystal shape and colour	Colourless, parallelepiped	Colourless, cuboid
Size (mm)	0.09 × 0.12 × 0.17	0.12 × 0.17 × 0.15
Lattice parameters, a, b, c	13.138 (2), 6.582 (1), 10.787 (2)	13.130 (2), 6.581 (1), 10.781 (1)
No. of reflections measured	9341	6375
$2\theta_{max}$ (°)	70	50
No. of unique observations	2086 > 3σ	2716 > 3σ
R_{int}	0.043	0.032
Max., min. transmission	0.4477, 0.2957	0.3495, 0.2576
Model	$RbTiOAsO_4$	$KTiOAsO_4$(W)
R (wR)	0.027 (0.031)	0.020 (0.025)
Exinction parameter	33 (2)	60 (2)
Flack enantiopole parameter	0.994 (1)	0.556 (9)
$\Delta\rho_{min}$, $\Delta\rho_{max}$ (e Å^{-3})	−1.5, +0.9 [near O(7)]	−0.8, +0.6 [near O(7)]

and crystals with $\mu R \approx 1$ were used, it was considered that the extra electron density was real. The effective occupancy of the Ti(2) site was refined for both sets of data, giving values of 1.088 (4) and 1.110 (5) for the arsenate- and tungstate-grown samples, respectively.

In the tungstate-grown crystal, the extra electron density on the Ti(2) site could be the result of incorporation of tungsten from the flux. The radius of octahedrally coordinated W^{6+} is closely matched to that of titanium so that this substitution is likely. This was corroborated by proton-microprobe measurements which did reveal some clustering of tungsten within the (100) section of tungstate-grown KTA. However, the fact that there is a peak of similar size in the arsenate grown sample suggests a more intrinsic origin of this effect. We suggest that both KTA crystals possess some disorder that it has not proved possible to resolve in these refinements. This manifested itself in earlier refinements using a $1/\sigma^2$ weighting scheme, as convergence of the K(1) and K(2) site occupancies to approximately 0.85 and 0.9, respectively. On the robust resistant refinement scheme reported here, both K(1) and K(2) site occupancies refine to 1 to within experimental error. The atomic parameters derived using the two different weighting schemes are the same. The only differences lie in some of the thermal parameters: compared with the parameters obtained from the $1/\sigma^2$ K-deficient model, U_{11}, U_{22} and U_{33} of K(1) increase by 15, 38 and 9%, respectively, with corresponding changes of 12, 8 and 1% in these parameters for K(2). The temperature factors of the O's generally decrease by 10–20%, but O(3) and O(4) become considerably more anisotropic because the U_{11} values are halved. For the K-deficient model, the Ti(2) occupancy refines to only 1.07 in the tungstate-grown crystal and 1.03 in the arsenate-grown crystal, suggesting that there is some correlation between the K-site occupancies and the residual density at Ti(2): also note that O(3) and O(4), which are the O's most affected by the choice of the fully stoichiometric model, are bonded to Ti(2) in the $P(1)O_4$–$Ti(2)O_6$ chains that run along the [100] direction.

The Flack enantiopole parameter (Flack, 1983) was refined for both samples with values of 0.99 (2) for the tungstate-grown sample, indicating that it was a single-domain crystal, and 0.556 (9) for the arsenate grown sample, indicating that it was a twinned sample with close to a 1:1 ratio of domains of opposite structural polarity. This result is consistent with the presence of polar twinning on a fine spatial scale in arsenate-grown KTA as the sample that was used for data-collection was only 150 μm in diameter.

Discussion of the structure

The atomic coordinates and anisotropic temperature factors obtained from the refinement of the data from the arsenate-grown sample are given in Table 2. (Those from the tungstate-grown sample are the same to within the estimated standard deviations.) The bond lengths and angles around Ti and As are given in Table 3. The distortions of the TiO_6 octahedra in KTA are smaller than that of the corresponding octahedra in KTP. The difference between the Ti(1)—O(5) long bond and the Ti(1)—O(6) short bond is 0.222 (4) Å and that between the Ti(2)—O(5) short bond and the Ti(2)—O(6) long bond is 0.288 (4) Å. These should be compared with the corresponding values in KTP, which are 0.265 (4) and 0.359 (4) Å, respectively. The range of bond

angles in the As(1)O_4 and As(2)O_4 groups is the same as was found by El Brahimi & Durand (1986), but the As—O bond lengths show a much smaller spread, particularly for the As(1)O_4 group.

Even though the individual groups that make up the framework of KTA are less distorted than their counterparts in KTP, the program *MISSYM* (Le Page, 1988) measures the whole framework as more distorted than the KTP framework. The use of this program to discuss the deviation of the room-temperature KTP structure from its high-temperature *Pnan* prototype symmetry has been discussed extensively before (Thomas, Glazer & Watts, 1990; Thomas *et al.*, 1992). The deviation is represented by a maximum tolerance in Å. These are 0.19 and 0.22 Å for KTP and KTA, respectively.

Because this tolerance is not in itself informative about the source of the increased distortion in the structure, the shifts of all the atoms from their projected high-temperature positions were calculated individually, as has been explained in previous publications (Thomas *et al*, 1990; Thomas & Glazer, 1991). For the atoms As(1), As(2), Ti(1) and Ti(2), which go to special positions in the prototypic phase, the shifts of the corresponding atoms in KTA and KTP agree to within the estimated errors, except for that of Ti(1) which is 0.045 Å in KTA and only 0.004 Å in KTP. The O atoms also show increased displacements from their high-temperature symmetry in KTA. These are most pronounced for the pairs of atoms O(7) and O(8), and O(9) and O(10), for which the displacements in KTA are almost double those in KTP. These atoms are all bonded to As(2), the more distorted of the two tetrahedra. Therefore, the increased maximum tolerance required for *MISSYM* to find the pseudo-symmetry elements in the KTA structure is associated with the atoms Ti(1) and O(7)—O(10).

When the environment of the As(2)O_4 tetrahedron is examined, it is found that there is a buckling of the framework in the vicinity of As(2), possibly associated with the exaggerated movement of Ti(1) relative to its high-temperature position. This is reminiscent of the changes in the KTP structure at high pressure (Allan, Loveday, Nelmes & Thomas, 1992). Of the Ti—O—P angles linking chains of TiO_6 octahedra and PO_4 tetrahedra in the framework, the P(2)—O(9)—Ti(2) bond angle shows an exaggerated decrease of 5° under pressure, whereas the other linking angles show changes of *ca* 2° only. When the Ti—O—As(2) linking angles involving O's bonded to

Table 3. *Bond lengths* (Å) *around* Ti *and* As

The symmetry operators given refer to the O atoms.

Around Ti(1)		Around Ti(2)	
O(1^{i})	2.126 (3)	O(3)	2.028 (2)
O(2^{ii})	1.967 (3)	O(4^{v})	1.990 (2)
O(5^{iii})	1.966 (3)	O(5^{vi})	1.787 (3)
O(6^{iv})	1.744 (3)	O(6)	2.075 (3)
O(7^{iv})	2.047 (3)	O(9^{vi})	1.967 (3)
O(8^{iii})	1.997 (3)	O(10)	1.988 (3)
Around As(1)			
O(1)	1.661 (3)	O(7)	1.681 (2)
O(2)	1.692 (3)	O(8)	1.676 (3)
O(3)	1.691 (2)	O(9)	1.701 (3)
O(4)	1.690 (2)	O(10)	1.681 (3)

Symmetry codes: (i) $x, y, z-1$; (ii) $-x+1, -y+1, z-\frac{1}{2}$; (iii) $-x+\frac{1}{2}, y-\frac{1}{2}, z-\frac{1}{2}$; (iv) $-x+\frac{1}{2}, y+\frac{1}{2}, z-\frac{1}{2}$; (v) $x-\frac{1}{2}, -y+\frac{1}{2}, z$; (vi) $-x+\frac{1}{2}, y-\frac{1}{2}, z+\frac{1}{2}$.

Table 2(*a*). *Atomic positions*

	x	*y*	*z*
K(1)	0.37725 (9)	0.7802 (1)	0.6856 (1)
K(2)	0.10748 (7)	0.6977 (2)	0.9288 (1)
Ti(1)	0.37445 (4)	0.50584 (8)	−0.00233 (8)
Ti(2)	0.24717 (4)	0.26783 (7)	0.74776 (8)
As(1)	0.49807 (3)	0.33035 (4)	0.74007 (8)
As(2)	0.18139 (2)	0.50645 (5)	0.48803 (7)
O(1)	0.4871 (2)	0.4948 (4)	0.8562 (3)
O(2)	0.5066 (2)	0.4659 (5)	0.6072 (2)
O(3)	0.3939 (2)	0.1822 (4)	0.7214 (3)
O(4)	0.5988 (2)	0.1738 (4)	0.7599 (3)
O(5)	0.2206 (2)	0.9569 (5)	0.3601 (2)
O(6)	0.2177 (2)	0.0555 (5)	0.6101 (2)
O(7)	0.1081 (2)	0.3057 (4)	0.4517 (2)
O(8)	0.1057 (2)	0.7065 (4)	0.5160 (3)
O(9)	0.2620 (2)	0.5414 (5)	0.3664 (2)
O(10)	0.2596 (2)	0.4648 (5)	0.6088 (2)

Table 2(*b*). *Anisotropic atomic displacement parameters*

	U(11)	*U*(22)	*U*(33)	*U*(23)	*U*(13)	*U*(12)
K(1)	0.0404 (6)	0.0160 (4)	0.0357 (5)	−0.0033 (4)	−0.0105 (4)	0.0037 (4)
K(2)	0.0175 (4)	0.0253 (4)	0.0404 (5)	0.0008 (4)	−0.0002 (4)	0.0052 (3)
Ti(1)	0.0045 (2)	0.0047 (2)	0.0060 (2)	−0.0006 (2)	0.0002 (2)	−0.0003 (2)
Ti(2)	0.0035 (2)	0.0064 (2)	0.0056 (2)	0.0019 (2)	−0.0009 (1)	−0.0007 (1)
As(1)	0.0040 (1)	0.0063 (1)	0.0069 (1)	−0.0004 (2)	0.0070 (9)	−0.0002 (1)
As(2)	0.0069 (1)	0.0047 (1)	0.0068 (1)	0.0007 (1)	−0.0005 (1)	−0.0005 (1)
O(1)	0.013 (1)	0.014 (2)	0.012 (1)	−0.0070 (9)	0.003 (1)	−0.0039 (9)
O(2)	0.007 (1)	0.015 (1)	0.014 (1)	0.007 (1)	0.0021 (9)	0.0031 (9)
O(3)	0.0046 (9)	0.010 (1)	0.015 (2)	−0.0006 (9)	−0.0023 (9)	−0.0003 (7)
O(4)	0.0044 (9)	0.009 (1)	0.015 (2)	0.0032 (9)	−0.0009 (9)	−0.0006 (7)
O(5)	0.005 (1)	0.012 (1)	0.011 (1)	0.001 (1)	0.0027 (8)	0.001 (1)
O(6)	0.015 (1)	0.009 (1)	0.011 (1)	−0.004 (1)	−0.0049 (9)	0.001 (1)
O(7)	0.010 (1)	0.0036 (9)	0.017 (2)	−0.0018 (9)	−0.0036 (9)	−0.0035 (8)
O(8)	0.014 (1)	0.008 (1)	0.017 (2)	0.002 (1)	0.005 (1)	0.0021 (9)
O(9)	0.010 (2)	0.013 (1)	0.009 (1)	0.0050 (9)	0.0049 (9)	0.004 (1)
O(10)	0.013 (2)	0.010 (1)	0.012 (1)	0.0050 (9)	−0.007 (1)	−0.004 (1)

As(2) in the KTA structure are examined, they are found to range from 124.55 [Ti(2)—O(9)—As(2)] to 132.69° [Ti(1)—O(8)—As(2)]. By contrast, the Ti—O—As(1) angles lie in the much smaller range 126.35–129.81°, which is comparable to the range found for the Ti—O—P angles in the KTP structure at ambient temperature and pressure.

Therefore, it appears that the accommodation of the larger As atom in the structure exerts an influence comparable to the effect of external pressure on the KTP framework. In particular, there is a severe distortion of the linkages around the AsO_4 tetrahedron with the Ti(2)—O(9)—As(2) angle taking an anomalously low value.

Non-linear optical topographs and etching

Loiacono & Stoltzenberger (1988) have described the formation of topographs using the second-harmonic signal generated by a crystal. These are capable of revealing the presence of domain boundaries, flaws and other optically inhomogeneous regions. Regions of opposite polarity can be distinguished because the d_{ijk} coefficients of the second-order susceptibility change sign under reversal of the sense of the polar axis. Neighbouring domains scatter out of phase and contrast is produced in the second-harmonic generation topograph at the boundary. Although pure KTA does not phase-match for 1.06 μm Nd:YAG radiation, sufficient second-harmonic at 532 nm can be generated from a thin section of KTA to allow examination of the crystals in this way.

(100) sections of tungstate- and arsenate-grown KTA were illuminated with a *Q*-switched Nd:YAG laser. The intensity distribution at the second-harmonic wavelength was recorded on photographic plates. The typical pattern generated (Fig. 1) from a tungstate-grown crystal shows two streaks inclined to one another. One of the streaks, that running approximately parallel to [010], is diffuse. The other, on closer examination, reveals a large degree of structure on a fine scale. The arsenate-grown crystals show broadly the same features, but the fine structure is absent. These features appeared only in the non-linear optical regime, *i.e.* in the second-harmonic generation. Normal illumination with light sources at different wavelengths (HeNe laser at 632.8 nm, frequency-double Nd:YAG at 532 nm and white light) did not reveal any unusual features in the linear optical regime.

To test the hypothesis that the structure in the patterns is related to the presence of domains, (100) and (001) sections cut from the same crystals were etched in H_3PO_4 at 353 K, as reported by Loiacono *et al.* (1992). Series of fine parallel lines were revealed on both surfaces of all four sections, but they did not appear to correlate with the structure in the SHG topographs. Evidence of twinning of a polar nature was not revealed by this etch.

In the tungstate-grown crystal, refractive index inhomogeneities associated with the uptake of tungsten in growth striae are a possible source of the structure in the SHG topograph. In the arsenate-grown sample, it is less easy to identify a possible contaminant, although there is evidence from the structural work of extra density on the Ti site which is consistent with the idea of compositional and, therefore, optical inhomogeneity. Although there has been much speculation about the presence of polar domains in KTA crystals grown from various fluxes, the only evidence that we have so far for their existence is the observation that the Flack parameter refined to 0.566 (9) for the arsenate-grown sample.

Non-linear optical properties of KTA

The non-linear optical polarization developed at the doubled frequency is given by

$$P_i(2\omega) = d_{ijk} E_j(\omega) E_k(\omega),$$

where d_{ijk} is a component of the non-linear optical (NLO) susceptibility and $E_j(\omega)$ and $E_k(\omega)$ are components of the optical field at the fundamental frequency. It has been well documented that the d_{ijk} components can be calculated from the vector sum

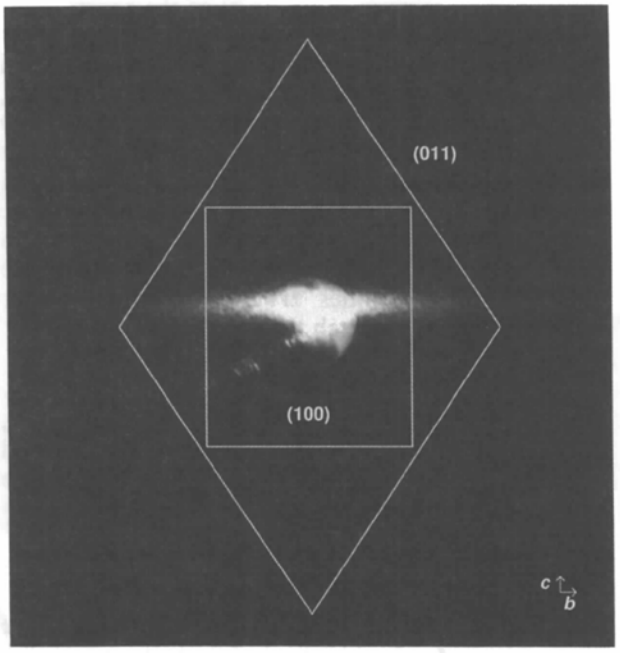

Fig. 1. An SHG topograph in transmission through a (100) section of a tungstate-grown KTA crystal overlaid with a schematic of the typical morphology of an as-grown crystal. The diffuse streak is almost parallel to (010) and the streak containing the fine structure is seen to be approximately normal to (011).

of NLO susceptibilities of individual bonds using a bond-polarizability model (Levine, 1972; Jeggo & Boyd, 1970).

The intrinsic non-linearity of a crystal is well represented by Δ_{ijk} coefficients defined by

$$\Delta_{ijk} = (d_{ijk})/(\varepsilon_0 \chi_{ii}^{2\omega} \chi_{jj}^{\omega} \chi_{kk}^{\omega}), \quad (1)$$

where χ_{ii} are the appropriate linear optical susceptabilities at the doubled and fundamental frequencies. On the bond-polarizability model, Δ's are given by

$$\Delta_{ijk} = \sum_{b=0}^{n} (g_{ijk}^{b} \Delta^{b})/V, \quad (2)$$

where V is the unit-cell volume, n is the number of bonds of type b in the unit cell, Δ^b is the individual non-linear Δ of a bond of type b and g_{ijk}^b is the geometric contribution of bond b to the non-linear coefficient (given by the appropriate product of direction cosines: $g_{ijk}^b = \cos \nu_i^b \cos \nu_j^b \cos \nu_k^b$).

This model has been employed in discussing the major structural contributions to the NLO response in KTP and its analogues (Hansen, Protas & Marnier, 1988; Zumsteg *et al.*, 1976), with the principal emphasis being on the unbalanced NLO response of the short Ti—O bonds of the highly distorted octahedra. The resultant response of a TiO_6 group depends on (1) the absolute magnitude of the non-linear susceptibilties of the bonds (Δ^b) and (2) the geometrical arrangement of the bonds expressed through the cosine products (g_{ijk}) of the short, intermediate and long Ti—O bonds. In KTA, the short Ti—O bonds are longer than their counterparts in KTP, indicating that their Δ^b's are smaller. However, Σg_{ijk} for the short, intermediate and long Ti—O bonds are almost identical in KTP and KTA, so that in the geometrical part only, the TiO_6 octahedra contribute in an identical fashion to the summations.

Δ_{ijk} must be scaled by the linear susceptibilities in order to obtain the calculated d_{ijk} coefficients [see (1)]. The susceptibilities are related to the linear refractive indices through the equations

$$\chi_{ii} = n_i^2 - 1,$$

where n_i are the principal refractive indices (i = 1, 2, 3). Changes in the refractive indices at the doubled and fundamental frequencies feed directly into the calculated non-linear optical coefficients. To illustrate the effect, $\Sigma(G_{ijk}/V)$ for the short bonds only in KTA and KTP have been scaled by the appropriate refractive indices (Table 4). Calculated d_{ijk} for KTA enhanced over the KTP by between 10 and 20% are obtained. Therefore, everything else being equal, the increase in refractive indices alone predicts larger d_{ijk} coefficients in KTA.

The most reliable published values of the NLO coefficients of KTA and KTP are gathered in Table 5. It is seen that d_{113} and d_{311} are enhanced by 20% and 10%, respectively, in KTA, whereas d_{333} and d_{322} are the same as the KTP values to within the errors. (d_{223} is estimated as 88% of the KTP value, but since this measurement was made on a Sc-doped KTA crystal, this may not provide a reliable comparison.)

Table 4. *Measured d_{ijk} in KTP and KTA*

d_{ijk}	KTP* d_{ijk} (pm/V)	KTA† d_{ijk} (pm/V)	Observed ratio, KTA:KTP
d_{113}	1.91	2.29	1.2
d_{223}	3.64	3.209‡	0.88
d_{333}	16.9	16.2 (1)	0.96
d_{322}	4.35	4.2 (4)	0.96
d_{311}	2.54	2.8 (3)	1.10

* Taken from Vanherzeele & Bierlein (1992).
† Taken from Cheng *et al.* (1993).
‡ Measured on a scandium-doped KTA crystal.

Only d_{113} and d_{311} show enhancements of a magnitude consistent with the refractive index changes, indicating that severe suppression of the NLO response is occurring by some other mechanism for the remaining coefficients. The geometrical contributions to d_{113} and d_{311} are identical, although they are scaled at different combinations of refractive indices (Table 6); similarly, d_{322} and d_{223}. In all KTP isomorphs, the d_{113} coefficient is dominated by the $Ti(1)O_6$ octahedron and the d_{223} coefficient is dominated by the $Ti(2)O_6$ octahedron. In particular, the d_{113} (d_{311}) coefficient is dominated by the Ti(1)—O(6) short bond and the d_{223} (d_{322}) coefficient by the Ti(2)—O(5) short bond. The corollary of this is that the Ti(1)—O(6) bond makes virtually no contribution to d_{223} and the Ti(2)—O(5) bond gives a negligible contribution to d_{113}. This can easily be understood from the crystal structure (Fig. 2): Ti(1)—O(6) lies almost parallel to (010) and has only a small component along **b**, whereas Ti(2)—O(5) lies almost parallel to (100) and has a small component along **a**. It is also expressed in the relative magnitudes of g_{ijk} for the contributions of the short Ti—O bonds to the d_{113} and d_{223} coefficients (Table 7).

Note that $Ti(1)O_6$ and $Ti(2)O_6$ are corner-linked through the O(5) and O(6) atoms so that the bisecting planes of the octahedra containing the O(5)—Ti(1)—O(6) and O(6)—Ti(2)—O(5) bond angles, respectively, are almost orthogonal; this has previously been described as a *cis–trans* arrangement. This bisecting plane in $Ti(1)O_6$ (Fig. 2) is almost parallel to (010), whereas that in $Ti(2)O_6$ is closely parallel to (100). The full analysis of the consequences of this orthogonality for the NLO properties of crystals of the KTP family will be given in a further publication.

The relevance of these observations to the NLO response of KTA in particular is as follows. In KTA, the Ti(1)—O(6) bond is 1.744 (3) Å, whereas the Ti(2)—O(5) bond is 1.787 (3) Å, considerably longer

Table 5. *Contribution of short* Ti—O *bonds to* g_{ijk} *for KTA and KTP*

ijk	KTP g_{ijk}/V (nm^{-3})	KTA g_{ijk}/V (nm^{-3})
113	1.716	1.604
223	1.660	1.508
333	2.712	2.784
322	1.660	1.508
311	1.716	1.604

Table 6. g_{ijk}/V *scaled by refractive indices for KTP and KTA*

d_{ijk}	*KTP**	*KTA**	*Ratio*
d_{113}	1.83	2.09	1.14
d_{223}	1.82	2.03	1.11
d_{333}	4.06	4.92	1.21
d_{322}	1.86	2.09	1.12
d_{311}	1.87	2.17	1.16

* All g_{ijk}/V are also scaled by a constant factor $C = \alpha/\varepsilon_o \Delta_b$ to bring them on to the same scale as the observed values. Δ_b is the bond polarizability of the short Ti—O bond, ε_o the permitivity of free-space and α a numerical constant.

Table 7. g_{ijk} *for* Ti(1)—O(6) *and* Ti(2)—O(5) *short bonds in KTP, illustrating orthogonal contributions to* d_{113} *and* d_{223} *coefficients*

	$g_{113} = g_{311}$	$g_{223} = g_{322}$	Dominant contribution to
Ti(1)—O(6)	−0.3523	−0.0131	d_{113} (d_{311})
Ti(2)—O(5)	−0.0259	−0.3494	d_{223} (d_{322})

than the 1.716 and 1.733 Å bonds in KTP. The non-linear susceptibility of a bond is a steep function of bond length. We suggest that the d_{113} (d_{311}) coefficient sees a KTP-like structure dominated by a short-bonded Ti(1)O_6 unit, whereas the d_{223} (d_{322}) coefficient sees a Ti(2)O_6 unit with a considerably weaker NLO response because of the increase in length of the Ti(2)—O(5) bond. Accordingly, the d_{113} and d_{311} coefficients, which are dominated by the Ti(1)—O(6) bond, increase in KTA by factors broadly consistent with the increased refractive indices, whereas the d_{223} and d_{322} coefficients are suppressed.

The orthogonality of the octahedra has also been commented upon in a very recent publication by Cheng, Cheng, Harlow & Bierlein (1994) on Nb-doped KTP. They also find unequal changes in the d_{113} and d_{333} coefficients relative to d_{223}, which they associate with unequal changes in the Ti(1)O_6 and Ti(2)O_6 octahedra in the Nb-doped structures. The full details of their structure refinements and their optical modelling has not been published so far and, therefore, we cannot say whether their findings for Nb:KTP are in agreement with ours for KTA. However, the similarity of the two approaches lends support to the ideas put forward here.

In order to test this hypothesis further, it is necessary to calculate the individual Ti—O bond susceptibilities from first principles. Sastry (1991) has calculated the linear susceptibilities of the Ti—O, P—O and K—O bonds in KTP using the methods of Shih & Yariv (1982), but our initial attempt to duplicate these results is not in agreement with Sastry's findings and further calculations are ongoing. Although our discussion has concentrated on Ti—O bonds, we have also considered the effect of As—O bonds in the structure. Engel & Defregger (1991) have calculated values for the P—O and As—O linear and non-linear bond susceptibilities in quartz-homeotypic structures. The calculated non-linear susceptibility of the As—O bond is approximately a factor of three times that of the P—O bond, so that the contributions of the AsO_4 tetrahedra are potentially significant when comparing KTA and

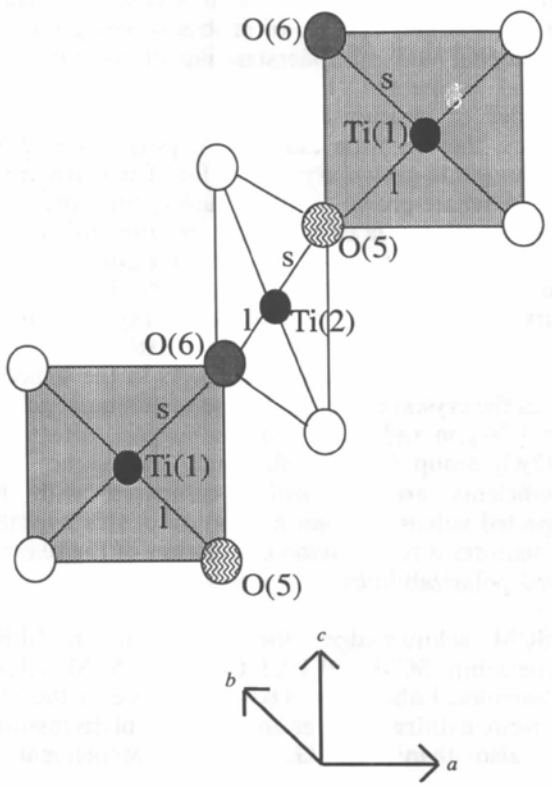

Fig. 2. A schematic diagram showing how the octahedra are linked in the KTA structure. The 'long' and anomalously short Ti—O bonds that are made in linking the octahedra (not drawn to scale on the figure) are marked by **l** and **s**, respectively. The plane of the Ti(1)O_6 octahedron which contains O(5), Ti(1) and O(6) is shown, and that of the Ti(2)O_6 octahedron containing O(6), Ti(2) and O(5). These planes are orthogonal (hence the description of these octahedra as having a *cis–trans* arrangement). The Ti(1)—O(6) short bond lies almost in the (010) plane, whereas the Ti(2)—O(5) short bond is confined to the (100) plane. The two Ti(1)O_6 octahedra shown are separated by half a unit-cell translation along **c**.

KTP. However, $\sum g_{ijk}$ for the AsO_4 tetrahedra are a factor of ten smaller than those for the Ti—O short bonds so that their contributions are constrained to be relatively small by geometry.

The principal refractive indices of KTA are increased by 0.0414, 0.0412 and 0.0439 from the KTP values. Using these structural data and the linear bond polarizabilities of Engel & Defregger (1991), we have also derived these changes from first principles and have accounted for the decrease in the optical anisotropy that results in the deviation of KTA from the phase-matching condition at 1.06 μm. These calculations will be described in detail in a future publication.

Concluding remarks

KTA is a potentially useful non-linear optical crystal. Although isostructural to KTP and therefore closely related to this material, it is slow to realise its potential largely because of problems with growth of the crystal and misunderstanding of its non-linear optical properties. From our experience with a number of crystals and different diagnostic techniques, there is little evidence of polar twinning in the tungstate-grown crystals so far. The fragment of the arsenate-grown crystal used for structure-determination was twinned, but etching and second-harmonic generation experiments on large plates of the same material did not show this in the bulk. Further X-ray anomalous scattering experiments are currently underway to settle this question.

The effect of substituting P by As in the structure takes the crystal out of the phase-matching condition for 1.06 μm radiation and, we suggest, affects the $Ti(2)O_6$ group in particular such that some NLO coefficients are diminished compared with the expected values. Further evaluation of this hypothesis requires a full *ab initio* calculation of the relevant bond polarizabilities.

SCM acknowledges the receipt of an SERC studentship. SCM and PAT thank Dr A. M. Glazer (Clarendon Laboratory, Oxford) for use of the Stoe four-circle diffractometer and for helpful discussions. We also thank Dr G. Grimes (Department of Nuclear Physics, Oxford) for the proton-microprobe measurements.

References

ALLAN, D. R., LOVEDAY, J. S., NELMES, R. J. & THOMAS, P. A. (1992). *J. Phys. Condens. Matter*, **4**, 2747–2760.
BIERLEIN, J. D., VANHERZEELE, H. & BALLMAN, A. A. (1989). *Appl. Phys. Lett.* **54**(9), 783–787.
CHENG, L. K., CHENG, L.-T., BIERLEIN, J. D., ZUMSTEG, F. C. & BALLMAN, A. A. (1993). *Appl. Phys. Lett.* **62**(4), 346–348.
CHENG, L. T., CHENG, L. K., HARLOW, R. L. & BIERLEIN, J. D. (1994). *Appl. Phys. Lett.* **64**, 155–157.
CRENNELL, S. J., CHEETHAM, A. K., JARMAN, R. H., THRASH, R. J. & KADUK, J. A. (1992). *J. Mater. Chem.* **2**(4), 383–386.
EL BRAHIMI, M. & DURAND, J. (1986). *Rev. Chim. Miner.* **23**, 146–153.
ENGEL, G. F. & DEFREGGER, S. (1991). *Phys. Status Solidi B*, **163**, 389–400.
FLACK, H. D. (1983). *Acta Cryst.* A**39**, 876–881.
HANSEN, N. K., PROTAS, J. & MARNIER, G. (1988). *C. R. Acad Sci.* **307**(II), 475–479.
JANI, M. G., MURRAY, J. T., PETRIN, R. R., POWELL, R. C., LOIACONO, D. N. & LOIACONO, G. M. (1992). *Appl. Phys. Lett.* **60**(19), 2327–2329.
JEGGO, C. R. & BOYD, G. D. (1970). *J. Appl. Phys.* **47**, 4980.
LE PAGE, Y. (1988). *J. Appl. Cryst.* **21**, 983–984.
LEVINE, B. F. (1972). *Phys. Rev. B*, **7**(6), 2600–2626.
LOIACONO, G. M., LOIACONO, D. N., ZOLA, J. J., STOLZENBERGER, R. A., MCGEE, T. & NORWOOD, R. G. (1992). *Appl. Phys. Lett.* **61**(8), 895–897.
LOIACONO, G. M. & STOLZENBERGER, R. A. (1988). *Appl. Phys. Lett.* **53**, 1499–1450.
MORRIS, P. A., FERRETTI, A. & BIERLEIN, J. D. (1991). *J. Cryst. Growth*, **110**, 697.
PERKINS, P. E. & FAHLEN, T. S. (1987). *J. Opt. Soc. Am. B*, **4**, 1066.
SASTRY, P. U. M. (1991). *Solid State Commun.* **78**(7), 593–597.
SHIH, C.-C. & YARIV, A. (1982). *J. Phys. C*, **15**, 825–846.
STOE & CIE (1988). *REDU4. Data Reduction Program.* Version 6.2. Stoe & Cie, Darmstadt, Germany.
THOMAS, P. A. & GLAZER, A. M. (1991). *J. Appl. Cryst.* **24**, 968–971.
THOMAS, P. A., GLAZER, A. M. & WATTS, B. E. (1990). *Acta Cryst.* B**46**, 333–343.
THOMAS, P. A., MAYO, S. C. & WATTS, B. E. (1992). *Acta Cryst.* B**48**, 401–407.
TORDJMAN, I., MASSE, R. & GUITEL, J. C. (1974). *Z. Kristallogr.* **139**, 103–115.
WATKIN, D. J., CARRUTHERS, J. R. & BETTERIDGE, P. W. (1985). *CRYSTALS User Guide.* Chemical Crystallography Department, Univ. of Oxford, England.
VANHERZEELE, H. & BIERLEIN, J. D. (1992). *Opt. Lett.* **17**, 982.
ZUMSTEG, F. C., BIERLEIN, J. D. & GIER, T. E. (1976). *J. Appl. Phys.* **47**, 4980.